

The Proper Motion of the Globular Cluster NGC 6553 and of Bulge Stars with HST¹

M. Zoccali², A. Renzini², S. Ortolani³, E. Bica⁴, B. Barbuy⁵

ABSTRACT

WFPC2 images obtained with the Hubble Space telescope 4.16 years apart have allowed us to measure the proper motion of the metal rich globular cluster NGC 6553 with respect to the background bulge stars. With a space velocity of $(U, \Theta, W) = (-3.5, 230, -3)$ km s⁻¹, NGC 6553 follows the mean rotation of both disk and bulge stars at a Galactocentric distance of 2.7 kpc. While the kinematics of the cluster is consistent with either a bulge or a disk membership, the virtual identity of its stellar population with that of the bulge cluster NGC 6528 makes its bulge membership more likely. The astrometric accuracy is high enough for providing a measure of the bulge proper motion dispersion and confirming its rotation. A selection of stars based on the proper motions produced an extremely well defined cluster color-magnitude diagram (CMD), essentially free of bulge stars. The improved turnoff definition in the decontaminated CMD confirms an old age for the cluster (~ 13 Gyr) indicating that the bulge underwent a rapid chemical enrichment while being built up at in the early Universe. An additional interesting feature of the cluster color-magnitude diagram is a significant number of blue stragglers stars, whose membership in the cluster is firmly established from their proper motions.

Subject headings: Astrometry; Globular clusters: individual: NGC 6553; The Galaxy: kinematics and dynamics;

1. INTRODUCTION

The globular cluster system of the Milky Way has a slightly bimodal metallicity distribution, and it was been suggested that the metal rich group ($[\text{Fe}/\text{H}] > -0.8$) would constitute a population of “disk” globular clusters (Zinn 1985; Armandroff

1989). These clusters are actually strongly concentrated towards the Galactic center, with most of them being physically inside the Galactic bulge, at a galactocentric distance $\lesssim 3$ kpc (see e.g., Fig. 3 in Zinn 1985). Much progress has been made in recent years in the study of this group of clusters, thanks to higher angular resolution CCD and near-infrared photometry and high resolution spectroscopy. The kinematics, vertical scale height, and metallicity distribution of these clusters turn out to be indistinguishable from those of the bulge field stars (Minniti 1995; Barbuy et al. 1998, 1999b; Côté 1999), leaving little doubt that they constitute a family of bulge, rather than disk globular clusters (see also Harris 2000 for a recent discussion).

Among these clusters, the best studied ones are the “twin” clusters NGC 6553 and NGC 6528 which have virtually identical color-magnitude diagrams (Ortolani et al. 1995). The subject of the present investigation, NGC 6553 ($\alpha=18:09:15.6$,

¹This work is based on observations with the NASA/ESA Hubble Space Telescope, obtained at the Space Telescope Science Institute, operated by AURA Inc. under contract to NASA

²European Southern Observatory, Karl Schwarzschild Strasse 2, D-85748 Garching bei München, Germany; mzoccali@eso.org, arenzini@eso.org

³Università di Padova, Dipartimento di Astronomia, Vicolo dell'Osservatorio 5, I-35122 Padova, Italy; ortolani@pd.astro.it

⁴Universidade Federal do Rio Grande do Sul, Dept. de Astronomia, CP 15051, Porto Alegre 91501-970, Brazil; bica@if.ufrgs.br

⁵Universidade de São Paulo, Dept. de Astronomia, CP 3386, São Paulo 01060-970, Brazil; barbuy@orion.iagusp.usp.br

$\delta = -25:54:28$, $l = 5^\circ 25'$, $b = -3^\circ 02'$, is a moderately concentrated (central surface brightness: $\log \Sigma = 4.53 L_\odot pc^{-2}$; Djorgovski 1993) globular cluster located at ~ 3 kpc from the Galactic Center. Its metallicity is high, although the exact value is still a matter of debate: Barbuy et al. (1999a) and Coelho et al (1999) found $[Fe/H] = -0.5$, while Cohen et al. (1999) measured $[Fe/H] = -0.16$. The first CCD photometry in the *BVRI* bands showed clear metal-rich characteristics, with the pronounced *V* band luminosity turnover of the upper Red Giant Branch (RGB) towards cooler temperatures, an effect of strong TiO blanketing (Ortolani et al. 1990). Subsequent *VI* data obtained with the Hubble Space Telescope (HST) by Ortolani et al. (1995; see also Guarnieri, Renzini & Ortolani 1997; Guarnieri et al. 1998) reached more than 3 magnitudes below the turnoff, leading to the conclusion that NGC 6553 is nearly coeval to the halo globular clusters. Still, the very high contamination by background stars around the cluster turnoff was very high, leaving some uncertainty on the value of the turnoff luminosity M_V^{TO} . The more recent study by Sagar et al. (1999) over a larger field ($6' \times 10'$) allowed them to obtain a cleaner cluster population by statistical subtraction of background stars. However, their data are not deep enough to allow photometry of turnoff stars with the accuracy required to address the problem of the cluster age.

Using a technique pioneered by King et al. (1998), in the present work we combine HST wide field and planetary camera (WFPC2) data from two epoch observations of the central regions of NGC 6553. Thanks to the excellent astrometric performances of WFPC2, we measure the relative proper motion of the cluster with respect to the bulge. This allows us to *i*) decontaminate the CMD of NGC 6553 from the background and therefore to obtain a more reliable measure of its age; *ii*) obtain the three components of the cluster space velocity; and *iii*) measure the bulge proper motion dispersions along Galactic longitude and latitude.

2. OBSERVATIONAL DATA AND ANALYSIS

We analyse two sets of observations of the central region of the bulge globular cluster NGC 6553,

taken with a time interval of 4.16 years. Both sets were collected with HST using the WFPC2 camera, with the filters F555W (*V*) and F814W (*I*). The first epoch data were acquired by our group on February 1994, as part of the GO5436 program (Ortolani et al. 1995; Guarnieri et al. 1997). Those of the second epoch were collected in April 1998, as part of the GO7307 program, and were retrieved from the HST archive. The log of observations for the two epochs is shown in Table 1.

Since the datasets were taken for independent purposes, they cover two fields which do not completely overlap. Figure 1 shows the relative orientation of the mosaics. Black dots show all stars detected in the WFPC2 mosaic in the first epoch observations: the size of the symbol is proportional to the star's brightness. The cluster center is located approximately at pixel (932,682). Overplotted on this map is the location of the WFPC2 mosaic of the second epoch observations, where the cluster is centered on WF3. This configuration, coupled with the different limiting magnitudes of the two observation sets, implies that only about 1/3 of the stars detected in the first epoch data have a counterpart in the second epoch photometry and could be used for astrometric purposes.

All images were de-biased, dark corrected and flatfielded through the standard HST pipeline. Following Silbermann et al. (1996), we have masked out the vignetted region, the saturated and bad pixels and columns using a vignetting mask, together with the appropriate data quality file for each frame.

The photometric reduction of each dataset was carried out using the DAOPHOT II/ALLFRAME

TABLE 1
LOG OF OBSERVATIONS

Program	Date	Filter	Exp. (s)
GO5436	25.2.1994	F555W	14
		F555W	2×100
		F814W	5
		F814W	2×50
GO7307	24.4.1998	F555W	3×5
		F555W	3×200
		F814W	3×20
		F814W	3×200

package (Stetson 1987, 1994). Preliminary photometry was performed on each single frame in order to obtain an approximate list of stars for each of them. The coordinates of the stars in common were used for an accurate spatial match among the different frames. With the coordinate transformations, we then obtained a single image, which is the median of all the frames, regardless of the filter. In this way we removed all the cosmic rays and obtained the highest signal-to-noise image for star finding. The DAOPHOT/FIND routine was applied to the median image and Point Spread Function (PSF) fitting photometry was carried out, in order to obtain the deepest list of stellar objects, free from spurious detections. Finally, this list was used as input to ALLFRAME, for the simultaneous profile fitting photometry of individual frames. The PSFs that we used were the WFPC2 model PSFs extracted by P. B. Stetson (1995, private communication) from a large set of uncrowded and unsaturated images. It is worth emphasizing that the photometric reductions of the two datasets were carried out separately.

The quality of the first epoch photometry turned out to be better than that of the second epoch, even if the total exposure time for each filter was longer in the second epoch data. The difference in the quality of the photometry in the two epochs is likely to be due to a combination of two effects: the worsening with time of the charge transfer efficiency loss of the WFPC2 chips, and the fact the adopted model PSFs, being obtained in 1995, reproduced the actual PSF of the first epoch better than the second. In what follows we will base our analysis on the 1994 photometry, while the spatial information from the 1998 data combined to that of 1994 will be used for the relative proper motion derivation.

Calibration of the HST instrumental magnitudes to the Landolt system was performed following the prescriptions by Dolphin (2000). These are an update of the widely used Holtzman et al. (1995) equations, including the most recent correction for the charge transfer efficiency loss. In principle, since the HST filter passbands are different from the Landolt ones, the recommended procedure to transform the instrumental magnitudes into the standard ground-based system is to subtract the absolute extinction in the instrumental bands *before* applying the transformations

(Holtzman et al. 1995). However, in this case no dereddening correction has been applied to our instrumental magnitudes, because we were mainly interested in producing a CMD as similar as possible to that of the ground-based photometries, and to derive the cluster reddening. The latter, in particular, is found to be strongly variable across the cluster area (Heitsch & Richtler 1999, see also Sect. 5) and therefore we would anyway subtract an inappropriate reddening to many stars.

3. THE COLOR MAGNITUDE DIAGRAM

Figure 2 shows the calibrated CMD extracted from the first epoch data. All the stars detected in the four WFPC2 chips are shown in this diagram. The most populated branches in this CMD are the cluster Main Sequence (MS), Red Giant Branch (RGB), and Horizontal Branch (HB): the latter being the inclined clump of stars at $V \sim 16.6$. The narrow sequence of stars at $V \sim 17.5$, which is almost parallel to the HB sequence is the RGB bump (Iben, 1968); as predicted by theory (e.g., Rood 1972), it is prominent in this metal-rich cluster. Both the RGB bump and the HB are shaped as an inclined sequence (instead of a clump) by differential reddening across the field (see below). Also clearly visible is the bulge RGB, which is about 0.5 magnitudes redder and ~ 1.5 mag fainter than the cluster RGB (the cluster is ~ 3 kpc closer to us along the line of sight than the bulk of the bulge field star population; (see below), being the cluster ~ 3 kpc closer to us compared with the bulk of bulge stars. The bulge Sub Giant Branch and turnoff region at $V \sim 21.5$ and $(V - I) \sim 2.1$ overlaps with the MS of NGC 6553. A well populated blue sequence departing from the cluster turnoff is also evident, and is expected to be a mixture of cluster blue stragglers and foreground disk stars.

For the astrometric calculations only those stars in common between the two epoch data, having photometric error smaller than 0.07 mag in both bands and shape parameter $-0.02 < \text{SHARP} < 0.05$ were selected. Polynomial 20-coefficient coordinate transformations were then calculated in order to take into account both the differences in the pointings and the distortion of the WFPC2 field. Figure 3 shows the residuals differences between the coordinates of the two epochs (epoch2-

epoch1). Obviously, since the astrometric transformations were constrained mainly by the much more numerous cluster stars, the residuals are, by definition, distributed around zero. Foreground and background (mostly bulge and some disk) stars, instead, are distributed around $(dx, dy) = (-0.23, 0.05)$ in this plot. Also shown in Fig. 3 are the directions of increasing Galactic longitude and latitude.

Figure 4 shows the result of the astrometric decontamination of the CMD. The left panel shows the CMD of only those stars which displacement between the two epochs lies inside a radius of 0.1 pixels centered on (0,0) in Fig. 3, which, as expected, are mainly cluster stars. Many cluster stars fall outside this circle, but such a small radius was chosen in order to select the cleanest sample of cluster stars. The right panel of Fig. 4 show the stars having proper motions $dx < -0.15$. Those are mainly bulge stars, with some residual contamination from cluster outliers.

4. PROPER MOTIONS AND SPACE VELOCITY

4.1. NGC 6553 Proper Motion

The distribution of the residuals shown in Fig. 3 allows us to determine both the relative proper motion of NGC 6553 with respect to the bulge, and the dispersion of the bulge proper motions along the two Galactic coordinates.

The former is the difference between the centroids of the bulge and cluster proper motion distributions, obtained by means of a Gaussian fit along both the l and b axis. Figure 5 shows the histograms of the dl and db distributions of both cluster and bulge stars. Note that the ratio of the integrals of the two Gaussians in Fig. 5 (lower left) also gives the relative number of bulge to cluster stars in the region of the WFPC2 field in common between the two epochs, which is 1400:7900=1:5.6. The relative motion of the cluster stars is by construction centered on $dl = 0$ and $db = 0$, while the bulge stars are clustered around $(dl, db) = (-0.245, -0.017)$ pixels, which corresponds to a relative proper motion of NGC 6553 with respect to the bulge of $\mu_l = 5.89$ and $\mu_b = 0.42$ mas yr⁻¹. Combining this result with the radial velocity of NGC 6553, $v_r = -6.5$ (Harris 1996, as updated on the WEB page:

<http://physun.physics.mcmaster.ca/Globular.html>), and adopting a Sun motion of $(U_\odot, V_\odot, W_\odot) = (10, 5.25, 7.17)$ km s⁻¹ (Dehnen & Binney 1998), the rotational velocity of the Local Standard of Rest of $V_{LSR} = 239$ km s⁻¹ (Arp 1986) and a cluster distance $d = 5300$ pc (see below) the three components of the NGC 6553 absolute space velocity are derived: $(\Pi, \Theta, W) = (-3.5, 230, -3)$ km s⁻¹ [Π points radially outwards from the Galactic center, W towards the North Galactic Pole and Θ is oriented in the direction of Galactic rotation]. This assumes that we measure all the background bulge stars, with those in the near side moving on average in the opposite direction with respect to those in the far side because of bulge rotation. Therefore, their *average* proper motion is zero. One concludes that NGC 6553 is describing a circular orbit close to the Galactic plane. Its rotational velocity is consistent with the mean rotation of the bulge at 2.7 kpc (Minniti 1995) but also with the disk rotation at the same distance (e.g. Amaral et al. 1996). Hence the kinematics of NGC 6553 appears to be consistent with either a disk or a bulge membership. However, its stellar population (age and metallicity) is identical to that of another metal rich cluster, NGC 6528 (c.f., Sec. 5), suggesting that the two objects have formed within the same environment (Ortolani et al. 1995). NGC 6528 is located at 1.3 kpc from the Galactic center, and its high radial velocity ($v_r = 185$ km/s; Harris 1996) clearly indicates that it is on a highly eccentric orbit, therefore excluding disk membership for this *bulge* cluster. All in all, both clusters appear to belong to the bulge population of globular clusters, with their kinematical properties being within the corresponding distribution for bulge stars.

4.2. Bulge Proper Motion Dispersion

The σ of the distributions shown in Figure 5 also allow the determination of the bulge proper motion dispersion. In order to reduce the contamination due to cluster stars in the determination of the bulge velocity dispersion σ_l along the axis of Galactic longitude, bona fide bulge stars were selected from the CMD as indicated in Fig. 5. The distribution of these stars in the (dl, db) plane (upper right panel) gives indeed a cleaner sample of bulge stars, with some residual cluster members, coming from the cluster lower main sequence. The

Gaussian fit to this distribution shown in the lower panels yields a better determination of the bulge proper motion dispersion: $\sigma_l = 0.119 \pm 0.012$ and $\sigma_b = 0.098 \pm 0.009$. The quoted uncertainties are the formal errors in the Gaussian fit of the histogram shown in Fig. 5. The fit was performed taking into account errors in both coordinates: the Poisson error for the y and the σ of the cluster Gaussian for the x . The dotted lines in the lower left panel are the two Gaussians whose sum is the solid line. The residual cluster component was fitted with a Gaussian with the same σ obtained from the fit of Fig. 5. Formally, the space velocity dispersion corresponding to the measured σ of the cluster stars is 28 km s^{-1} . We are not aware of any measurements of the velocity dispersion of NGC 6553, but in general globular clusters have velocity dispersions $< 10 \text{ km s}^{-1}$ (e.g., Pryor & Meylan 1993). Therefore, we conclude that the distribution of the cluster star in the (dl, db) plane is entirely due to observational errors. Deconvolving the latter from the observed dispersion of the bulge stars we finally obtain $\sigma_l = 2.63 \pm 0.29$ and $\sigma_b = 2.06 \pm 0.21 \text{ mas yr}^{-1}$. We therefore confirm the existence of a proper motion anisotropy $\sigma_l/\sigma_b = 1.28 \pm 0.19$ already found by many authors (e.g., Zhao, Rich & Biello, 1996, who measured $\sigma_l/\sigma_b = 1.15 \pm 0.06$ towards Baade’s Window) and interpreted as evidence of the mean bulge rotation. The values of the proper motion dispersions obtained from Fig. 6 for our field at $(l = 5.^\circ 25, b = -3.^\circ 02)$ are somewhat lower than the values $\sigma_l \sim 3.2$ and $\sigma_b \sim 2.7$ found both towards Baade’s Window $(l = 1^\circ, b = -4^\circ)$ and the Plaut’s Field $(l = 0^\circ, b = -8^\circ)$ (Spaenhauer, Jones & Whitford 1992; Rich & Terndrup 1997; Mendez et al. 1997).

5. THE DISTANCE AND AGE OF NGC 6553

The relative proper motion decontamination has provided a cleaner cluster CMD, but the sequences still show a significant width due to differential reddening (e.g. Heitsch & Richtler 1999). In the process of matching the overlapping regions of different frames in the two epochs data, the WFPC2 frame was divided into small sub-fields (e.g., part of the first epoch WF4 overlaps partly with the WF3 and partly with WF4 of the second epoch data). In these comparisons, it appeared that a region of the cluster mapped by the WF4

presents lower reddening, both absolute and differential, and its CMD has much narrower and bluer sequences. A fiducial ridge line extracted from it was used to apply the method described in Piotto et al. (1999) and obtain a cluster CMD partially corrected for differential reddening. The observed field was divided in 84 sub-fields of equal size and the CMD of each of them was shifted along the reddening line to overlap the fiducial sequence. The result is show in Fig. 7: the left panel shows the original cluster CMD, the central one is reddening-corrected and the right panel shows the fiducial line for 47 Tuc and NGC 6528 overplotted on that of NGC 6553.

The central and right panels of Fig. 7 allow a measure of age and distance with higher accuracy with respect to the previously available data. The estimated apparent magnitude of the cluster HB is $V^{\text{HB}} = 16.6 \pm 0.05$. Following Ortolani et al. (2000), we adopt $M_V^{\text{HB}} = (0.16 \pm 0.10) \times [\text{Fe}/\text{H}] + (0.98 \pm 0.10)$ and $[\text{Fe}/\text{H}] = -0.5 \pm 0.3$, giving $M_V^{\text{HB}} = 0.90 \pm 0.12$. The cluster apparent distance modulus is therefore $(m - M)_V = 16.60 - 0.90 = 15.70 \pm 0.13$.

The reddening is derived from comparisons to the 47 Tucanae locus (Ortolani et al. 1995; Kaluzny et al. 1997). The color of the RGB of NGC 6553 at the HB level is $V - I = 2.08 \pm 0.03$. With respect to 47 Tuc we derive $\Delta(V - I)_{(\text{NGC}6553-47\text{Tuc})} = 0.99$. Part of this color shift ($\Delta(V - I) = 0.134$, Girardi et al. 2000) is due to the metallicity difference between the two clusters. Indeed, 47 Tuc has metallicity $[\text{Fe}/\text{H}] = -0.76$ (Harris 1996) and $[\alpha/\text{Fe}] = 0.3$ (Gratton, Quarta & Ortolani 1986), therefore a global metallicity $[\text{M}/\text{H}] = -0.55$, while Coelho et al. (2000) measured $[\text{M}/\text{H}] = -0.1$ for NGC 6553. Assuming $E(V - I)_{47\text{Tuc}} = 0.05$ (Barbuy et al. 1998) we finally obtain $E(V - I)_{\text{NGC}6553} = 0.99 - 0.135 - 0.05 = 0.805$ and therefore $E(B - V) = E(V - I)/1.28 = 0.63$ and $A_V = 0.63 \times 3.3 = 2.08$. The adopted total-to-selective extinction ratio $R_V = 3.3$ ratio was assumed considering the metallicity and reddening amount dependences (Barbuy et al. 1998 and references therein). This value of the reddening is lower than previous determinations (and therefore the *apparent* distance modulus shorter) because the reddening corrected CMD has been registered on the fiducial line of a low-reddening re-

gion. The absolute distance modulus of NGC 6553 is $(m - M)_0 = 15.70 - 2.08 = 13.62$, in perfect agreement with the value $(m - M)_0 = 13.60$ found by Guarnieri et al. (1997), and corresponding to a heliocentric distance $d = 5.3$ kpc.

Figure 7 also shows the fiducial line of 47 Tuc and NGC 6528 (Ortolani et al. 1995) overplotted on that of NGC 6553. The former two were shifted both in magnitude and in color in order to bring their upper MS into coincidence with that of NGC 6553. The extremely small differences in the TO and HB locations are well inside the uncertainty in the construction of the fiducial lines, from which we conclude that the three clusters are coeval to within ~ 1 Gyr, and therefore the absolute age of NGC 6553 (and NGC 6528) is ~ 13 Gyr as recently determined for 47 Tuc (Zoccali et al. 2001). This demonstrates that the Galactic bulge was enriched to solar abundance to within a rather short time scale (less than a few Gyr). The difference in the RGB slopes seen in the right panel of Fig. 7 is due to the difference in global metallicity of the three clusters. Note that the age-sensitive parameter $\Delta V_{\text{HB}}^{\text{TO}}$ changes by only a few hundredths of magnitudes in this metallicity range (see Fig. 3 of Rosenberg et al. 1999).

6. THE CLUSTER BLUE STRAGGLERS

As apparent from Fig. 4, at least part of the stars in the blue sequence above the cluster MS seem to belong to the cluster, hence they are probably blue stragglers (BS), rather than Galactic disk main sequence stars. This is confirmed by the following two experiments.

In order to check this issue, we isolated the probable BS stars in the decontaminated CMD (Fig. 8: left panel), and investigated their radial distribution as compared with the other cluster stars. The upper right panel of Fig. 8 shows that the cumulative distribution of the BS (dotted line) have the same spatial distribution as the cluster RGB (solid line) with $17.5 < V < 19.6$. This indicates that they are indeed cluster members. However, the BS population of NGC 6553 does not appear concentrated towards the center as they are in high density clusters (e.g., Ferraro et al. 1999). The second check on the BS nature of a major fraction of the blue sequence stars can be made by using their distribution of proper mo-

tions. This is displayed in the lower right panel of Fig. 8 which shows *all* the stars brighter than $V = 19.3$ and bluer than $V - I = 1.76$ in the original CMD (Fig. 2), and confirms that a large fraction of them are indeed concentrated around $(dx, dy) = (0, 0)$ and therefore are likely BS members of NGC 6553.

7. CONCLUSIONS

Using WFPC2 images taken 4.16 yr apart we have been able to measure both the proper motion of the globular cluster NGC 6553 and of the Galactic bulge stars in the background of the cluster. The main results obtained can be summarized as follows.

1. The cluster NGC 6553 appears to be on a nearly circular orbit ~ 3 kpc from the center of the Galaxy, with a velocity of ~ 230 km s $^{-1}$ and a small inclination with respect to the Galactic plane. These kinematical properties are consistent with both a bulge and a disk membership of the cluster. However, the cluster stellar population is virtually identical to that of the cluster NGC 6528, which kinematics makes its membership to the bulge unambiguous, and we conclude that also NGC 6553 is likely a member of the Galactic bulge.
2. The relative astrometry between the two epochs is accurate enough for measuring the dispersion of proper motions of bulge stars along the two Galactic coordinates, with $\sigma_l = 2.63$ and $\sigma_b = 2.06$ mas yr $^{-1}$.
3. The distinct proper motions of the cluster and bulge stars has allowed us to construct decontaminated CMDs for both the cluster and bulge populations. The resulting improved CMD for the cluster has allowed us to obtain more accurate values for the reddening, distance, and age of the cluster: NGC 6553 appears to have the same age as the inner halo globular cluster 47 Tuc (~ 13 Gyr) within a ~ 1 Gyr uncertainty. Given the high metallicity of both NGC 6553 and NGC 6528, this indicates that the Galactic bulge underwent rapid metal enrichment to solar metallicity and beyond, some 13 Gyr ago, supporting the view of an early and rapid assembly of the Galactic Bulge.
4. Thanks to the accurate astrometry obtained, we have also demonstrated that the cluster contains a significant population of blue stragglers, having separated them from a trace population of

stars with similar luminosities and colors which instead are likely intermediate age foreground disk stars.

We thank the referee, Patrick Côté, for useful comments. BB and EB acknowledge partial financial support from CNPq and Fapesp (Brasil). SO acknowledges the Ministero dell'Università e della Ricerca Scientifica e Tecnologica (MURST) under the program on 'Stellar Evolution' (Italy).

REFERENCES

- Amaral, L.H., Ortiz, R., Lépine, J.R.D., Maciel, W.J. 1996, MNRAS, 281, 339
- Armandroff, T.E. 1989, AJ 97, 375
- Arp, H. 1986, A&A, 156, 207
- Barbuy B., Bica E., Ortolani S. 1998, A&A, 333, 117
- Barbuy, B., Renzini, A., Ortolani, S., Bica, E., & Guarnieri, M.D. 1999a, A&A, 341, 539
- Barbuy B., Ortolani S., Bica E., Desidera S. 1999b, A&A 348, 783
- Coelho, P., Barbuy, B., Perrin, M.N., Idiart, T., & Schiavon, R.P., 2000, A&A, in preparation
- Côté, P., 1999, AJ, 118, 406
- Dehnen, W., & Binney, J.J. 1998, MNRAS, 298, 387
- Djorgovski, S. 1993, in Structure and Dynamics of Globular Clusters, eds. S. G. Djorgovski & G. Meylan (San Francisco: ASP), p. 373
- Dolphin A.E., 2000, PASP, 112, 1397
- Ferraro, F.R., Paltrinieri, B., Rood, R.T., Dorman, B., 1999, ApJ, 522, 983
- Girardi, L., Bressan, A., Bertelli, G., & Chiosi, C. 2000, ApJ, 530, 62
- Gratton, R.G., Quarta M.L., & Ortolani S. 1986, A&A, 169, 208
- Guarnieri, M.D., Renzini, A., & Ortolani, S. 1997, ApJ, 477, 21
- Guarnieri M.D., Ortolani S., Montegriffo P., Renzini A., Barbuy B., Bica E., Moneti A., 1998, A&A 331, 70
- Harris W.E. 1996, AJ 112, 1487
- Harris, W.E. 2000, Saas Fee Lectures 1998 (Berlin, Springer), in press
- Heitsch, F., & Richtler, T. 1999, A&A, 347, 455
- Holtzman J., Burrows C.J., Casertano S. et al., 1995, PASP 107, 1065
- Iben, I. Jr. 1968, ApJ, 154, 581
- Kaluzny, J., Krzeminski, W., Mazur, B., Wysocka, A., Stepień, K. 1997, Acta Astron., 47, 249
- King I.R., Anderson J., Cool A.M., Piotto G., 1998, ApJ, 492, L37
- Mendez, R.A., Rich, R.M., Van Altena, W.F., Girard, T.M., van den Berg, S., & Majewski, S., 1998, IAU Symp.
- Minniti, D., 1995, AJ, 109, 1663
- Ortolani S., Barbuy B., Bica E. 1990, A&A 236, 362
- Ortolani S., Renzini A., Gilmozzi R., Marconi G., Barbuy B., Bica E., Rich R.M. 1995, Nature 377, 701
- Ortolani, S., Momany, Y., Bica, E., & Barbuy, B., 2000, A&A, 357, 495
- Piotto, G., Zoccali M., King I.R., Djorgovski S.G., Sosin C., Rich R.M., Meylan G., 1999, AJ, 118, 1737
- Pryor, C., & Meylan, G., 1993, in ASP Conf.Ser.50, Structure and Dynamics of Globular Clusters, eds. S.G. Djorgovski and G. Meylan, (San Francisco: ASP), 357
- Rich, R.M., & Terndrup, D.M., 1997, in ASP Conf.Ser. 127, Proper Motions and Galactic Astronomy, ed. R.M. Humphreys, (San Francisco: ASP), 129
- Rood, R.T., 1972, ApJ, 177, 681
- Rosenberg, A., Saviane, I., Piotto, G., & Aparicio, A., 1999, AJ, 118, 2306
- Sagar, R., Subramaniam, A., Richtler, R., and Grebel, E.K. 1999, A&A, 135, 391
- Silbermann N.A., Harding P., Madore B.F., 1996, ApJ 470, 1
- Spaenhauer, A., Jones, B.F., & Whitford, A.E., 1992, AJ, 103, 297
- Stetson P.B., 1987, PASP 99, 191
- Stetson P.B., 1994, PASP 106, 250
- Zhao, H., Rich, R.M., & Biello, J., 1996, ApJ, 470, 506
- Zinn, R., 1985, ApJ, 293, 424

Zoccali, M., Renzini, A., Ortolani, S., Bragaglia,
A., Bohlin, R., Carretta, E., Ferraro, F.R.,
Gilmozzi, R., Holberg, J.B., Marconi, G., Rich,
R.M., Wesemael, F., 2001, ApJ, submitted

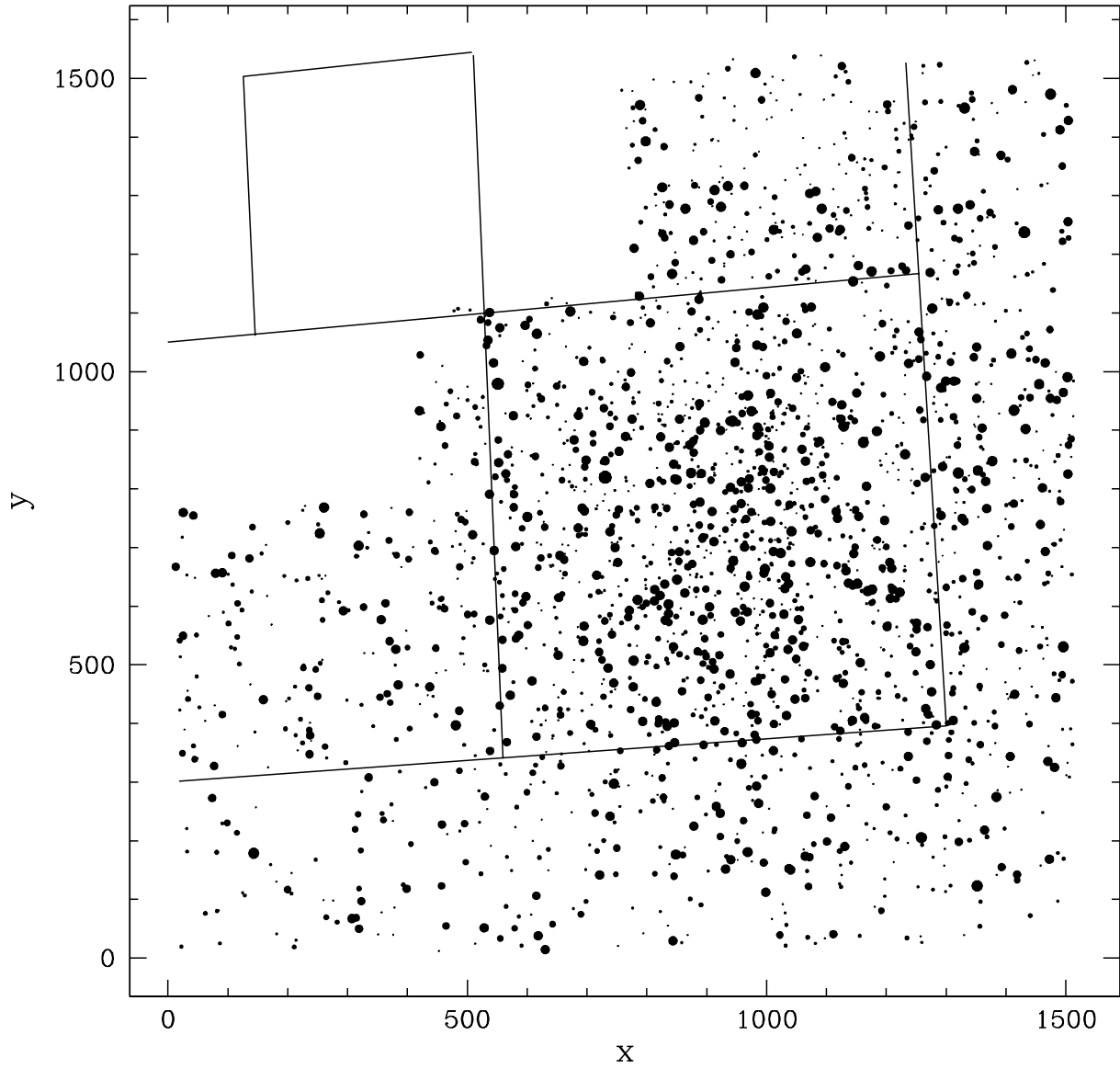


Fig. 1.— X, Y pixel map of NGC 6553: all stars detected in the WFPC2 mosaic in the first epoch observations are represented by black dots; symbol sizes are proportional to the stellar brightness. The location of the WFPC2 mosaic of the second epoch observations is overplotted on this map.

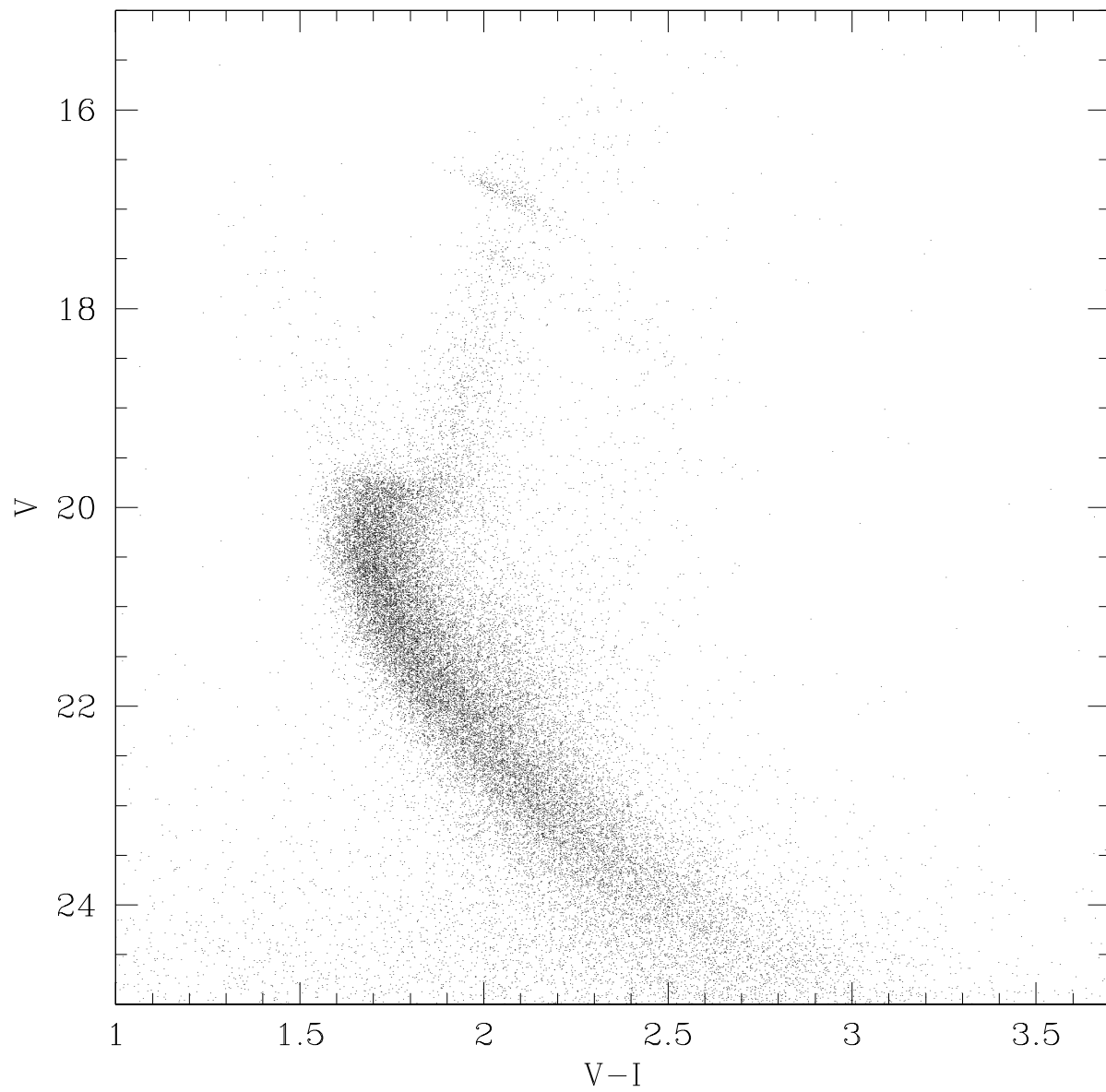


Fig. 2.— NGC 6553 calibrated CMD extracted from the four WFPC2 chips of the first epoch observations.

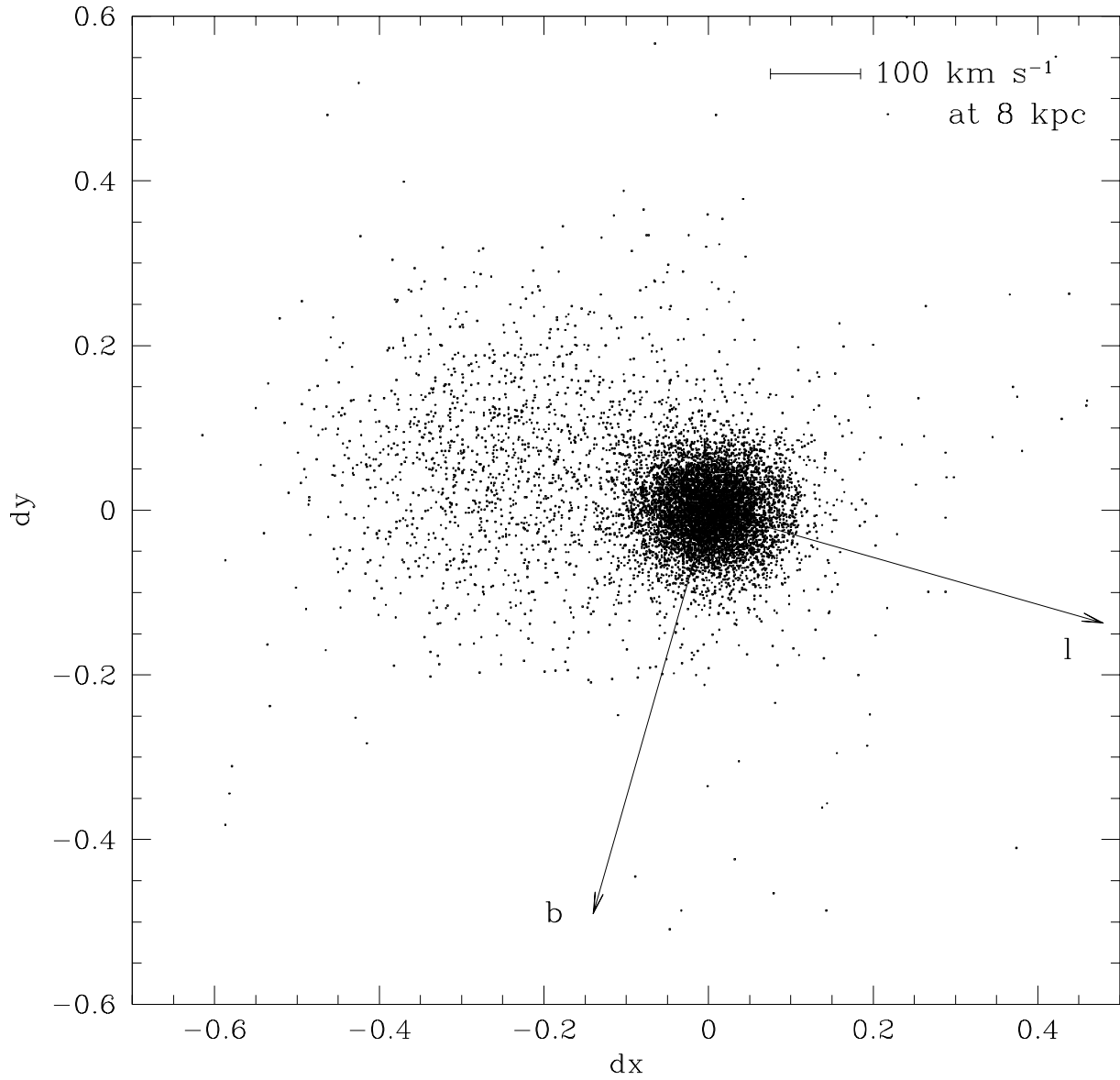


Fig. 3.— Relative proper motions (dx,dy) in pixels between the two epochs. The arrows show the direction of increasing Galactic longitude (l) and latitude (b).

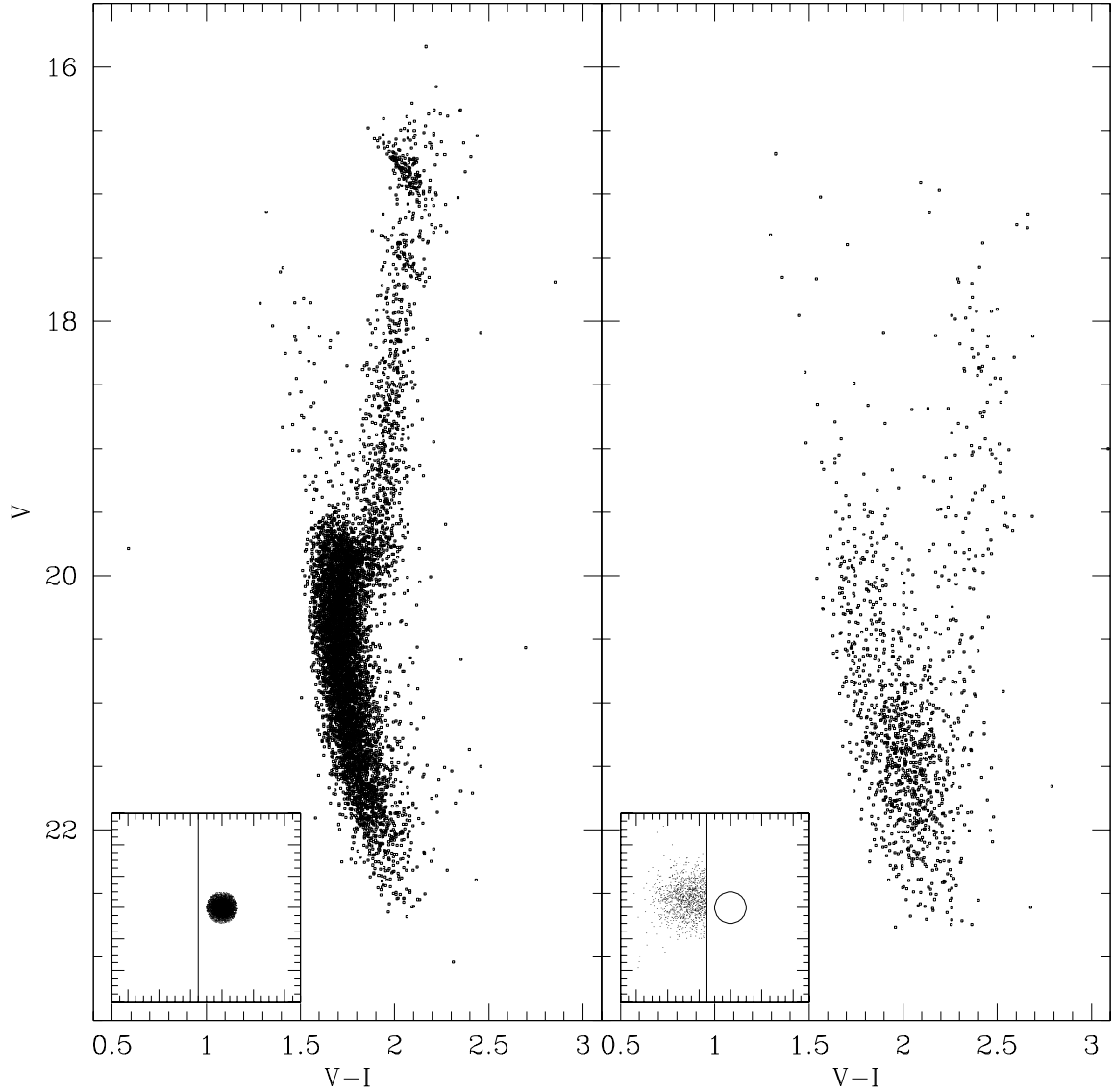


Fig. 4.— Left panel: NGC 6553 stars, selected as those lying inside a radius of 0.1 pixels centered on (0,0) in Fig. 3 (reproduced in the panel inset). We selected the stars inside a relatively small radius in order to obtain the cleanest possible cluster CMD. Right panel: CMD of (mainly) bulge stars, selected as those having $dx < -0.15$ in Fig. 3. Cluster stars are still present in this CMD because, being much more numerous, a still appreciable number of them fall well outside the selected cluster circle.

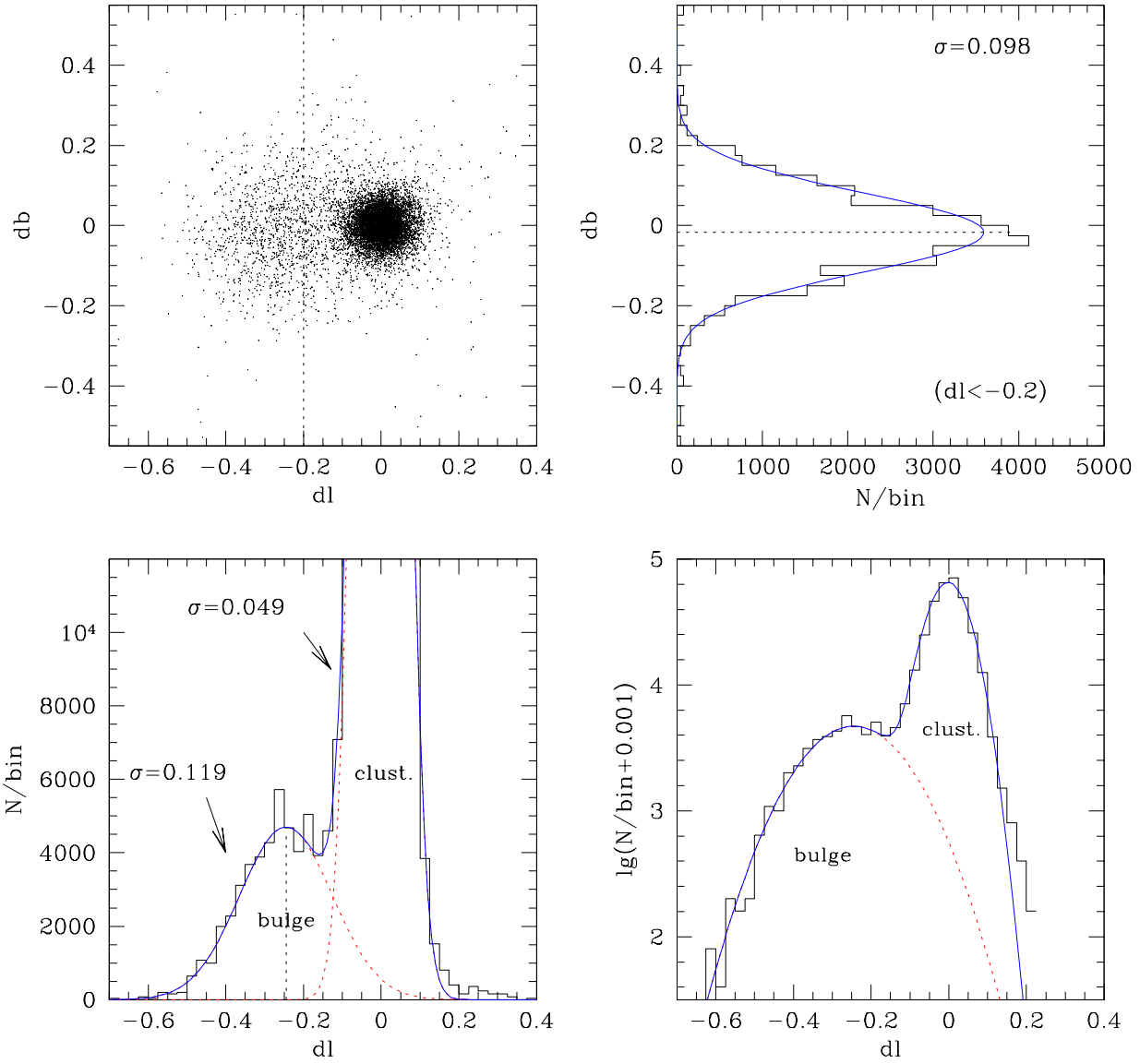


Fig. 5.— Upper left: Same as Fig. 3 now as a function of Galactic longitude and latitude. Upper right: Gaussian fit to the db distribution of stars with $dl < -0.2$ in the (dl, db) plane. Lower left: Gaussian fit to the dl distribution of all the stars. The dotted lines are the individual Gaussians while the solid line is their sum. Lower right: same fit plotted in logarithmic units.

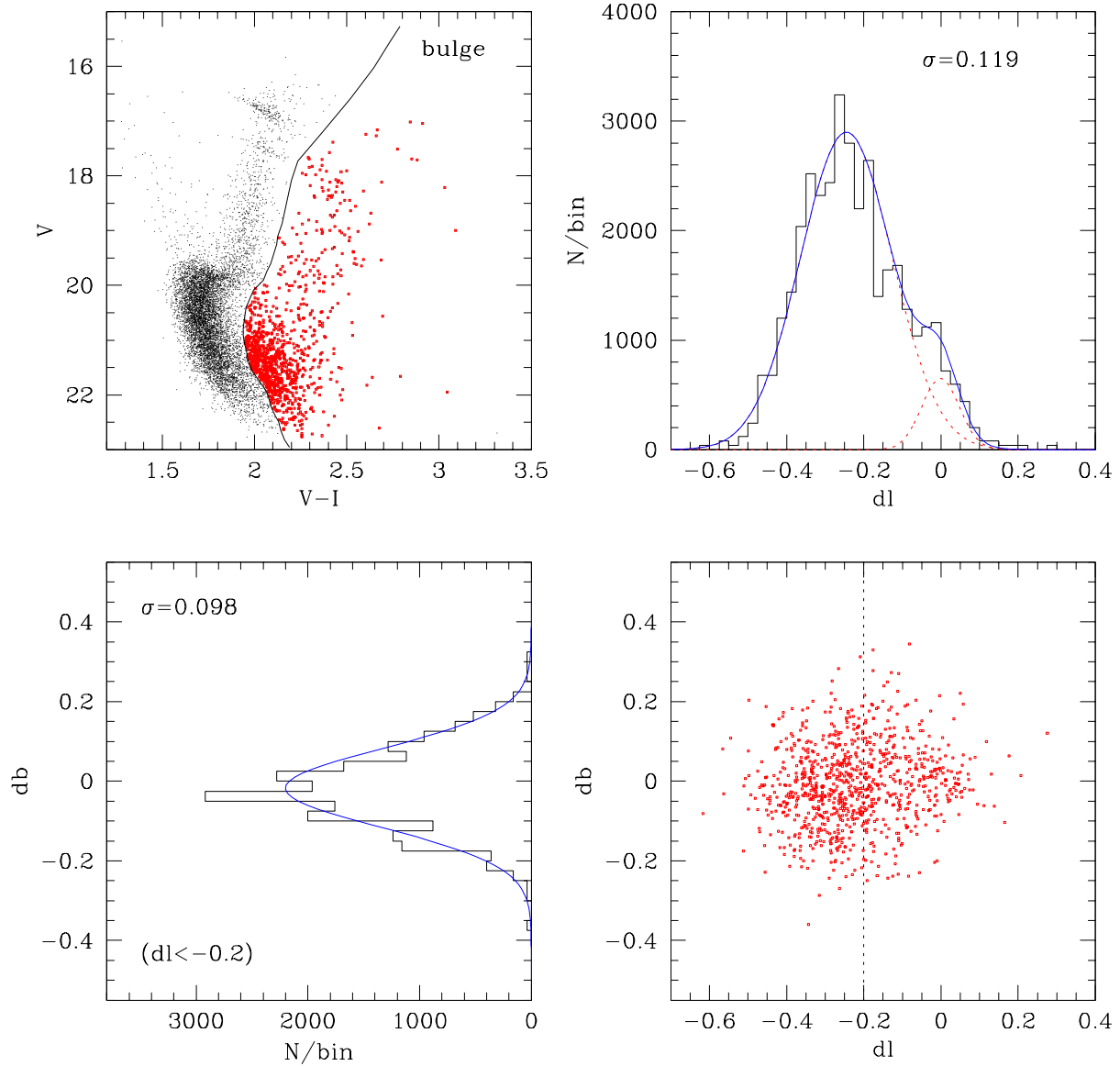


Fig. 6.— Upper left: bulge stars as selected from the CMD. Upper right: Gaussian fit to the dl distribution of all the stars selected from the CMD. Some residual cluster members are left and were fitted with a Gaussian with the same σ found in Fig. 5. The dotted lines are the individual Gaussians while the solid line is their sum. Lower left: same fit for the db distribution of stars having $dl < -0.2$. Lower right: (dl, db) distribution of the bulge stars selected from the CMD.

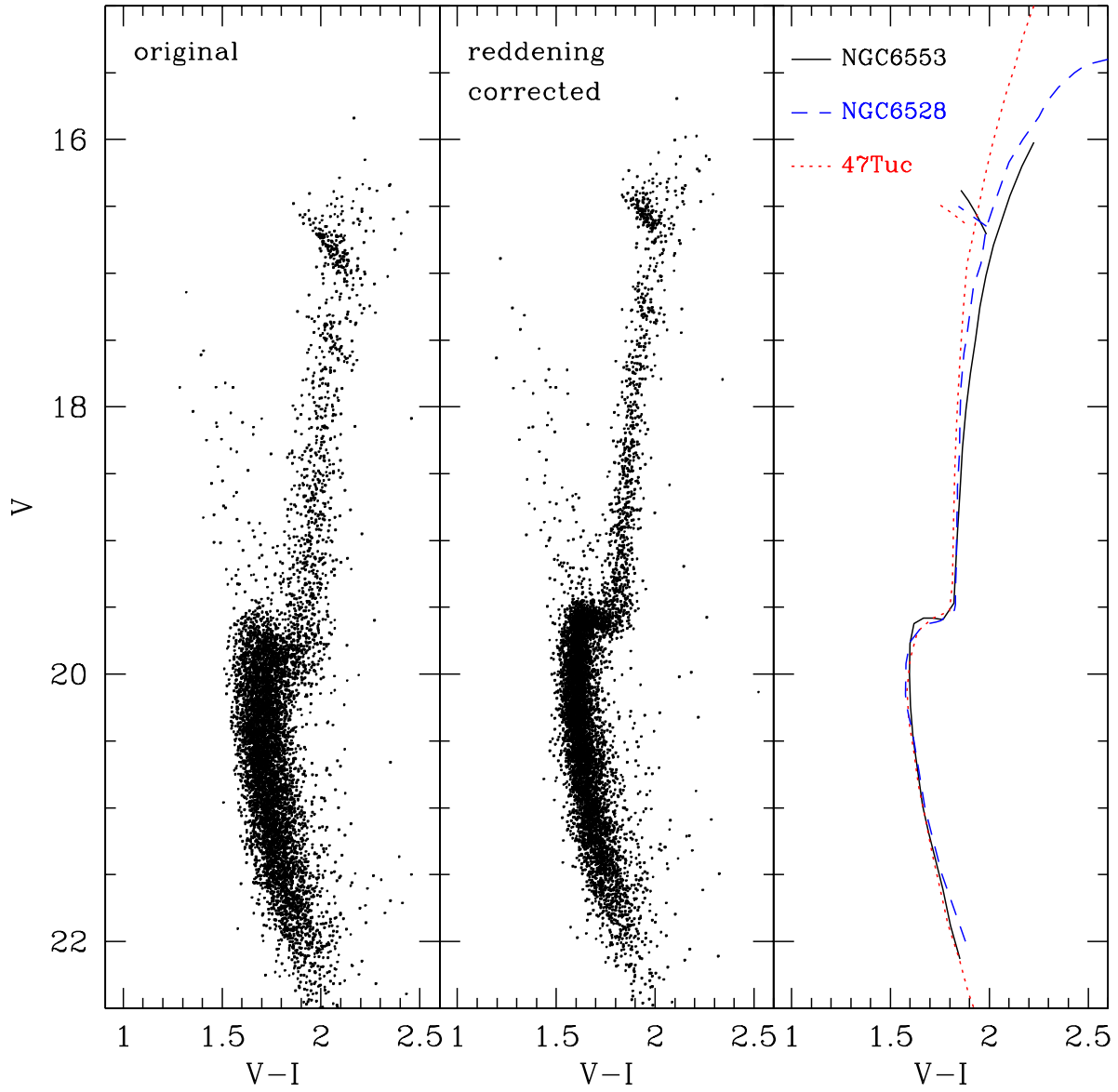


Fig. 7.— Left: original decontaminated CMD. Center: decontaminated CMD also corrected from differential reddening. Right: comparison between the fiducial lines of NGC 6553, NGC 6528 and 47 Tuc. The latter two have been shifted both in color and magnitude in order to overlap the MS and SGB of NGC 6553.

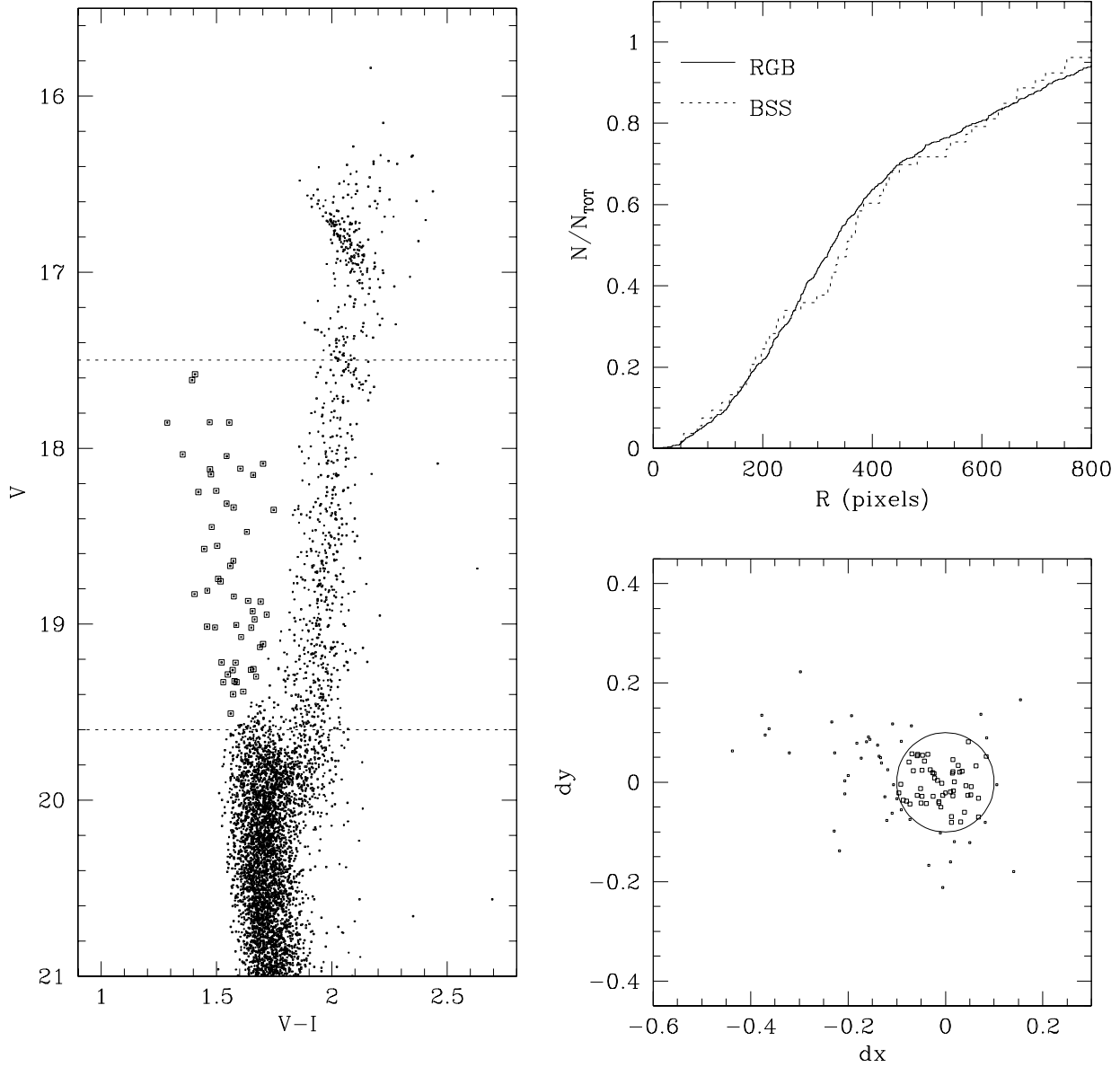


Fig. 8.— Left panel: The open squares indicate the candidate BS in the CMD of the likely cluster members, i.e., those stars with proper motion < 0.1 pixels. Upper right panel: cumulative radial distribution (in pixels) of the BS (dotted line) compared with the RGB stars (solid line) with $17.5 < V < 19.6$. Lower right: proper motion distribution of all the stars brighter than $V = 19.3$ and bluer than $V - I = 1.76$ in the original CMD. Note the strong concentration within the circle of 0.1 pixels radius, chosen to select the most likely cluster members.